ISSN: 0976-3104

SUPPLEMENT ISSUE
Barahmand and Mozhdeh

ARTICLE OPEN ACCESS

THE PROPERTIES OF FLOW AND FORCES APPLIED ON BRIDGE PIERS WITH DIFFERENT GEOMETRIES IN RIVER FLOW IN MEDIUM AND HIGH REYNOLD`S NUMBER IN DIFFERENT APPROACH ANGLES

Nader Barahmand*, Hamed Mozhdeh
Department of Civil Engineering, Larestan Branch, Islamic Azad University, Larestan, IRAN

ABSTRACT

The reduction of river profile due to the plants or other factors can create scour .The narrowing of flow stream in the location of bridge makes the water level rise in bridge upstream and increase of flow velocity. Consequently, the potential of deposit carrying or the river bed erosion intensity increases. in these cases , the erosion continues until the flow profile increases to the extent that the capacity of deposit carrying decreases becoming equal to that in bridge upstream and finally the erosion fails to continue. generally, the scour is created in hydraulic structure downstream , bridge piers and almost wherever scattered flow intensity increases locally. downstream area of separation where there are small and big eddies and the pressure is fixed is said to be wake. In laminate layer where the velocity is low, it is more likely for separation to happen than turbulent border layer. To investigate separation and its consequences on the bridge pier playing an important role in decrease or increase of scour. The range of Re is 10000 to 50000. The drag coefficient in all columns showed a decreasing trend versus Re. the drag of elliptical column had the lowest value. The greatest drag is related to square and column, the cylinder drag at high Re has a lower values than square and column which is due to pressure drag reduction from the movement of separation point to downstream resulting in smaller eddy behind the column and drag reduction.

Published on: 25th– Sept-2016

KEY WORDS

bridge pier, square column, rhombic column, drag, cylindrical column, rectangular column, turbulent flow, river flow

***Corresponding author: Email**: nader_barahmand@yahoo.com; **Tel:** +98-9177052312, +98-711-6254541, **Fax:** +98-711-6260909

INTRODUCTION

The scour and flow passing different geometrical forms of bridge pier have been paid attention to by many researchers. The formation of eddies behind the single and double cylinders becomes very important, too. Based on the studies of Larson et al (1961) pier form is an important factor which affects the scour depth because horse-shoe eddy depends on pier form. The rectangular pier makes the greatest depth of scour. Making the pier form compatible with flow lines to reduce the separation of flow decreases the scour depth so that in parallel case of pier form and flow lines, horseshoe eddy power decreases remarkably and less scour happens. If the pier front is in aerodynamic shape , the power of horseshoe eddy decreases and pier downstream is aerodynamic ,the eddy power decreases. [1 , 2]

Genes did some experiments on Harding model at scale 1/65 to determine the effect of upstream depth and diameter of bridge piers concluding that maximum scour depth occurs at pier tip and scour depth is 5 to 15% less around the pier while the ration of scour depth to flow depth has a direct relationship with flow speed. Flow depth of upstream has a direct effect on scour depth in pier tip. Parol et al, in their study on scour depth, understood if pier length is parallel with water flow , the scour depth will be minimum. With the increase of pier axis angle to flow line , the depth of scour will increase. In circular pier, the direct has no effect on scour. [3]

But if , instead of a pier, several piers are co-direction, the flow direction plays a role in increasing scour depth regarding the angle with pier axis. In this research , the fluid flow in rivers around the bridge pier is studied in different types. The flow analysis is carried out in different attack angles and Reynolds` number. [4]

MATERIALS AND METHODS

Calculation methods and conditions

The calculation is based on numerical method of finite volume elements. instable , viscous and unsteady flow is expressed in terms of 3-d equations of Noyer–Stoks .

$$\frac{\partial}{\partial t}(\rho \boldsymbol{V}) + \nabla.\rho\, \boldsymbol{VV} = \rho \boldsymbol{f} + \nabla.\Pi_{ij} \quad (1)$$

$$\frac{\partial \rho}{\partial t} + \nabla.(\rho \boldsymbol{V}) = 0 \quad (2)$$

In these equations , v and p are velocity and pressure, respectively. The second term on right represents the surface forces on volume unit, which are applied by external stresses including normal and shear stresses shown by stress tensor component. In this research, the 3-d time equations of basic pressure were used. [5] In the section of coupling velocity and pressure ,simple algorithm was used while in descreting the Least square cell based was applied and in pressure section ,the second order algorithm and in momentum part upstream second order descreting method were used. The descrete navier-stokes equations with simple methods was used as follows.

$$a_P u_P^* + \sum_{n=nb} a_n u_n^* = S_x - \Delta\Omega \frac{\partial P}{\partial x}$$
$$a_P v_P^* + \sum_{n=nb} a_n v_n^* = S_y - \Delta\Omega \frac{\partial P}{\partial y} \quad (3)$$
$$a_P w_P^* + \sum_{n=nb} a_n w_n^* = S_z - \Delta\Omega \frac{\partial P}{\partial z}$$

In which s is the product of momentum sink on volume unit in direction I in cell volume and coefficients a are calculated for interpolation of central subtraction .the descreted equations of direction x for adjacent cells of p and e are as follows:

$$u_P + (\frac{\Delta\Omega}{a_P})_P (\frac{\partial P}{\partial x})_P = (\frac{S_x}{a_P})_P - (\frac{1}{a_P} \sum_{n=nb} a_n u_n)_P \quad (4)$$

$$u_E + (\frac{\Delta\Omega}{a_P})_E (\frac{\partial P}{\partial x})_E = (\frac{S_x}{a_P})_E - (\frac{1}{a_P} \sum_{n=nb} a_n u_n)_E \quad (5)$$

The turbulence model in this research is k-e standard. In eddy viscosity k-e , the chaos field is expressed in two variables:

a) turbulent kinetic energy k [1] (relationship 6).
b) The turbulence equation in this method is as following: in standard model of ε[2] (relationship 7).
the values of k and e are obtained from semi-experimental methods:
:

$$K = \frac{1}{2}\overline{u_i' u_i'} \quad (6)$$

$$\varepsilon = \left(\frac{\mu}{\rho}\right)\overline{u_{i,j}' u_{i,j}'} \quad (7)$$

In which c1,c2 and c3 are experimental coefficients and σ_k and σ_k are turbulent prandtl and schmidt numbers.

The terms $c_1\left(\frac{\varepsilon}{k}\right)G$ and $c_2\left(\frac{\varepsilon^2}{k}\right)G$ are used for shear production and viscose decay processes

$$\rho\frac{\partial k}{\partial t} + \rho u_j k_{,j} = \left(\mu + \frac{\mu_t}{\sigma_k} k_{,j}\right)_{,j} + G + B - \rho\varepsilon \quad (8)$$

[1] Turbulent Kinetic Energy
[2] Viscous Dissipation Rate of Turbulent Kinetic Energy

$$\rho\frac{\partial k}{\partial t}+\rho u_j k_{,j}=\left(\mu+\frac{\mu_t}{\sigma_k}k_{,j}\right)_{,j}+G+B-\rho\varepsilon$$

The term ε shows the effect ε buoyancy. In this equation, the term $C_1(1-C_3)\frac{\varepsilon}{k}B$ represents the production G

turbulent kinetic energy from the interaction between the medium flow and turbulent flow field , as called shear production. The term B shows the buoyancy loss from fluctuating density field of flow. [6 , 7]
Exact relations for B and G are as follows:

$$G=-\rho\overline{u_i'u_j'}u_{i,j} \quad (9)$$

$$B=\overline{\rho' u_i'}g_i \quad (10)$$

For fixed density flows , the buoyancy term is obtained by Bozinsk approximation as follows :

$$B=\overline{\rho' u_i'}g_i \quad (11)$$

Reynolds` number is defined as the following:

$$\mathrm{Re}=\frac{\rho v c}{\mu} \quad (12)$$

IN THIS FORMULA, v IS THE FREE FLOW VELOCITY , ρ is free flow density, c is body reference level

and y is the cinematic viscosity. Here, μ is considered to be drag coefficient C_D is the surface covered by flow:

$$\mathrm{C_D}=\frac{\mathrm{D}}{2U_\infty^2 S} \quad (12)$$

Boundary conditions and calculation grid the coordinates system is considered to be Cartesian (x,y,z). the grid produced is a structure grid of hexahedron with a million meshes. In **[Figure–1],** different grids around the pier are shown. as seen, the produced grids are structured. The independence of results from calculation grid are shown in Reynolds` number 60000 and the wedged column was obtained at range, $-6d \le x \le 15d$, in which d is the cylinder diameter. For independency of results from time step , two steps of t= and t= , are taken. [8]

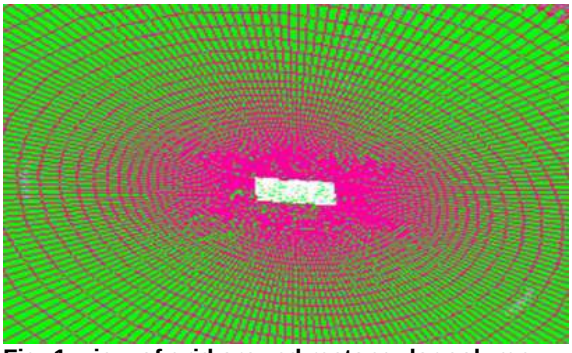

Fig: 1. view of grid around rectangular column

RESULTS

The results of solving flow around elliptical column in fluid in different angles

The contour of velocity, pressure, flow lines and eddy structure of flow at attack angle of 45 and different Reynolds` number are shown at . As seen, the maximum of velocity and pressure is at the pole and equinox of column.AS seen, increasing Reynolds` number increases the maximal velocity covering a larger area and due to flow velocity and flow asymmetry , the area of maximal velocity is different on both sides of cylinder. Also, maximum pressure is seen to be in front of column. Increasing the flow velocity increases the area of maximal pressure. As seen from

the pictures of flow lines around the object , increasing the Reynolds` number makes the left eddy larger than the right one due to the physical shape of the elliptical cylinder , causing inequality of force coefficient in x and y directions .At attack angle of zero degree , increasing Reynolds` number increases velocity and pressure reaching maximum at Reynolds` number of 70000. [9]

The contour of velocity , pressure, flow lines and eddy structure of flow at attack angle of 45 and different Reynolds` number are shown at **[Figure–2].**The flow around the column at 90 attack angle is symmetrical while the flow separates in the equinox area of column and eddy flow is produced. The maximal velocity is seen in the equinox of column , the maximal pressure in column front and stagnation point.Increasing Reynolds` number increases maximal and minimal velocity area. The separation area of flow becomes greater and a greater eddy sequence is formed behind the column. at Reynolds` number 150000 , the maximal velocity and pressure reach the maximum but the flow is symmetrical. [10]

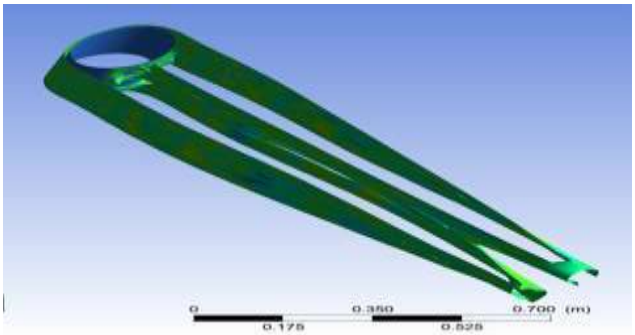

Fig: 2. Detection of eddy change behind Column using equivalent surfaces of rotation and Re=150000 and angle

DISCUSSION

The results of solving flow around square column in fluid in different angles

The contour of velocity, pressure, flow lines and eddy structure of flow at attack angle of 0 and different Reynolds` number are shown at figure in below.

As seen in Reynolds` number 10000, the momentary flow around the object is symmetrical and maximal velocity and pressure are formed in the column central corner and 90 corner of the beginning of the column. The flow separates from the corner in the middle of square column and two eddy sequences are formed behind the column. Increasing the Reynolds` number to 20000 increases the maximal velocity and maximal pressure and the length of eddy area behind the column increases. The flow is momentarily symmetrical. As seen, increasing Reynolds` number to 80000 , the maximal velocity reaches its peak and its area spreads to downstream. The eddy flow behind the column becomes more spread. The pictures taken are based on momentary velocity showing the asymmetry of flow around the column but the mean values of flow have symmetry. [11]

At the attack angle of 45 at Reynolds` number 10000, the maximal velocity occurs at two corners of column front but the flow does not separate and it separates in two rear corners. The maximal pressure occurs at surface center of column front. Increasing maximal velocity increases the velocity and pressure covering a greater area. Increasing Reynolds` number to 20000 , the separation of flow at the front corner of column starts due to the increase of velocity gradient but again it sticks to lateral surface and separates in two ending corners. As a result ,a small eddy is formed in two beginning corners of wing. Therefore, increasing Reynolds` number to 60000 , the maximal velocity and its area spread and the flow separates in the sharp corner of column front and two eddies larger than the previous one are formed in the lateral surface while the length of the eddy behind the column increases. Increasing Reynolds` number to 100000, the velocity and pressure increase remarkably .The separation area becomes spread in the corners of the column front and the pressure in the eddy area decreases to the lowest. Four eddies in lateral surfaces and back surfaces enlarge covering more area. **[Figure–3]**

THE IIOAB JOURNAL
ISSN: 0976-3104

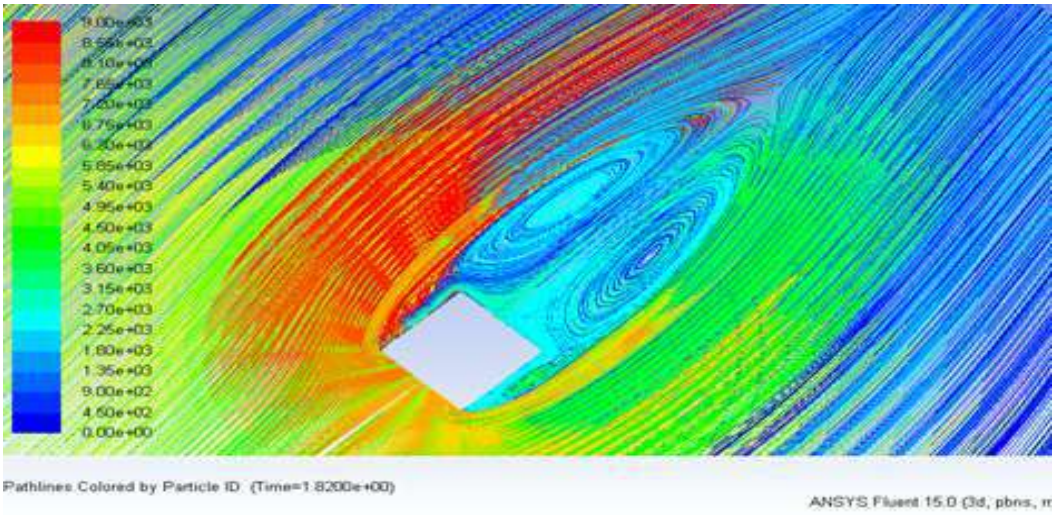

Fig: 3**. velocity contour around wedged column at 0 and re=10000**

As seen in at attack angle of zero, increasing Reynolds` number increases the maximal velocity occurring at two corners of wedge. As the velocity gradient increases in this place , there appears an eddy area behind the column in which velocity is very low. The highest pressure occurs at the top which is the stagnation point and the lowest at maximal velocity points.

Behind the wedge, the pressure decreases due to the eddy flow. Increasing Reynolds` number increases the maximal and minimal pressures. At attack angle of 45,the flow symmetry around wedged-like column disappeared relative to attack angle zero. The greatest velocity takes place at the tip of wedge and the ending corner. Increasing velocity increases the maximal velocity covering a greater area around the object. At the eddy area behind the object ,the pressure reaches minimum due to the eddy flow. The greatest pressure forms at the sides against the flow, the stagnation point, increased by the rise of velocity. as expected ,the pressure is negligible at eddy region. **[Figure–4]**

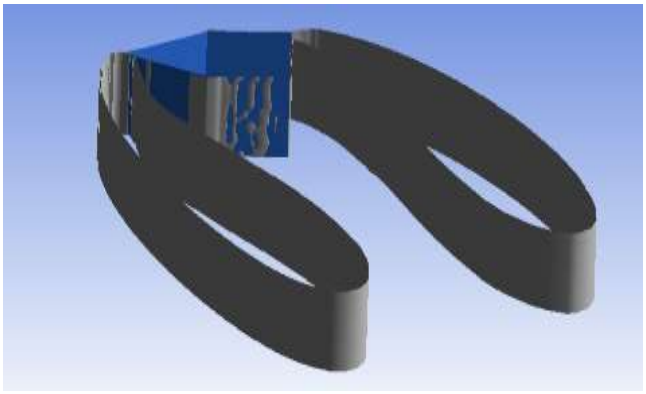

Fig: 4. velocity contour around wedged r column at 90 and re=10000

The contour of velocity and pressure around the wedged-like column at attack angle of 90 is seen in . the stagnation point of the corner flow is opposite the flow and maximal velocity happens at two corners opposite the flow in a small space. The maximal velocity and the included space increase with Reynolds` number. At the eddy area of separated flow behind the wedge, the velocity is negligible and the greatest pressure is at the stagnation point, increased by Reynolds` number. From the flow lines around the column, at Reynolds` number 10000, the separation occurs at right corner gradually and the flow sticks the surface at the end of lateral surface and once again separates. Increasing the Reynolds` number raises the separation area in the right corner of front surface and an eddy is formed at the surface which becomes spread with Reynolds` number and is attached to the eddy area behind the object, increased by rise of Reynolds`. [12]

The results of solving flow around round-tip cylindrical column in fluid in different velocities

The contour of velocity, pressure, flow lines and eddy structure of flow at different Reynolds` numberof 10000 to 50000 are shown at at figer in below. As seen, the maximum of velocity is at corner arc of flow in column.

The results of solving flow around cylidrical column in fluid in different velocities .As seen, the maximum of velocity is at the equinox of column. As seen in the figure, with the grid or organization , the border layer mash can be used more reliably, as in showing the organized mesh on border layer of pierr making optimization and cell modification better than disorganized mesh , in turn increasing accuracy and reducing the error. As corner opposite the flow has lower velocity gradient , the flow does not separate from the corners while attached to the surface without any eddy. the maximum and minimum of velocity are increased and cover a larger area the same as eddy behind the object. the greatest pressure is on stagnation point and its maximum pressure and area increases. Increasing Reynolds` number increases the extent of eddy area the results of solving flow around square column in fluid in different velocities.

The mesh grid around cylindrical pier is seen . As flow separation is important and there are formed specific trails behind the cylindrical piers , selection of grid and the number of points play important role in solving flow.

It is necessary to use organized mesh in border layer on pier to control increase or decrease the number of points on sphere surface and pier border layer so that separation site and forces are located carefully .shows the view of cylindrical pier on x-y direction. the symmetric conditions are in the top and bottom of the pier and wall conditions faraway and boundary conditions of velocity input and field exit were considered.

The volume of computational grid was about one million. the solution convergence and error are shown.

The contour of velocity , pressure, flow lines and eddy structure of flow at different Reynolds`

number of 10000 to 50000 are shown at. the results of solving flow around square column in fluid in different velocities. the flow around square pier is symmetric and the maximum velocity occurs at sharp corner opposite the flow. increasing Reynolds` number increases the velocity and enlarges the trails behind the column. the results of solving flow around round-tip cylindrical column in fluid in different angles. the contour of velocity, pressure, flow lines and eddy structure of flow at different Reynolds` numberof 10000 to 50000 are shown at figure in below.

As seen, the maximum of velocity is at corner arc of flow in column. AS seen, increasing Reynolds`number increases the maximal velocity covering a larger area and due to flow velocity and flow asymmetry , the area of maximal velocity is different on both sides of cylinder. Also, maximum pressure is seen to be in front of column. Increasing the flow velocity increases the area of maximal pressure. As seen from the pictures of flow lines around the object , increasing the Reynolds` number makes the left eddy larger than the right one due to the physical shape of the elliptical cylinder , causing inequality of force coefficient in x and y directions .At attack angle of zero degree , increasing Reynolds` number increases velocity and pressure reaching maximum at Reynolds` number of 70000. The greatest pressure forms at the side opposite the stagnation point and maximum pressure covers a great area. The increase of velocity increases the value and extent of this area. The pressure in eddy area is negligible.

The results of solving flow around cylidrical column in fluid in different angles .as seen, the maximum of velocity is at the equinox of column. as seen, increasing Reynolds` number increases the maximal velocity covering a larger area. the stagnation point occurs at pole opposite the flow and flow separation happens behind the cylinder , reduced by increase of velocity **[Figure–5].** the separation moves downstream with the increase of Reynolds` number.

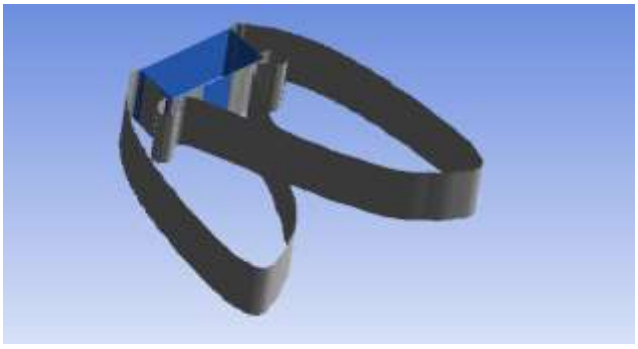

Fig: 5. change in elliptical column drag coefficient versus Reynolds number at attack angle 90

Comparison of drag change in columns

The change of drag coefficient interms of Reynolds number for elliptical column at 45 is seen. Drag coefficient decreases when Reynolds number increases as the separation point moves downstream reducing pressure drag and the total drag. At Reynolds` number 60000 to 80000 , there is a less reduction of Reynolds` number at higher Reynolds` number .The increase of friction drag has more effect on total drag while in lower Reynolds` number , increase of friction drag is due to the increase of flow contact surface and velocity has less effect on total drag. drag coefficient change to Reynolds` number of elliptical column at attack angle of 90 is shown. The drag coefficient decreases with the increase of Reynolds` number which is due to pressure drag reduction from separation point movement to downstream on column surface. [13]

The change of drag in wedged column at attack angle of 45 is seen. as flow separation takes place at two corners opposite the flow on wedged column, the drag reduction is due to reduction of total drag on the object from the flow becoming more aerodynamic on the object. the change of drag versus Reynolds` number is seen in **[Figure–6].**With the increase of Reynolds` number ,the drag decreases .The reduction of drag from Reynolds` number 30000 to 40000 experiences more gradient due to complete separation of flow which helps the flow around column to have more aerodynamic shape to reduce drag. for drag coefficient change on square column versus Reynolds` number at attack angle of 0, the flow separates from the two right angle corners opposite the flow unrelated to Reynolds` number. As the flow with stagnation pressure covers almost all the front surface, drag reduction from velocity increase is not tangible. The total drag reduction is due to total pressure behind the object due to eddy shape and increase of eddy length behind the object. at attack angle 45 drag decreases with increase in Reynolds` number continued to 40000.There is no remarkable change in drag of over re=4000 as the aerodynamic shape improves to re=40000 due to increase of eddy behind the object which reduces the drag. Drag coefficient change to Reynolds` number at attack angles 0 and 45 for square are presented. as seen, drag coefficient decreases with the increase of Reynolds` number. Drag coefficient change to Reynolds` number at attack angles 0,45 and for rectangular column are presented . as seen, drag coefficient decreases with the increase of Reynolds` number.

Comparison of drag change in columns

In rectangular column, coefficient change at three attack angle of 0,45 and 90 are compared. in which drag coefficient increases with the increases of attack angle.

From **[Figure–6],** rectangular column drag is less than that of wedged column. from drag of square column is greater than that of rectangular column in all reynolds` number which is due to the trails behind the rectangular column reducing total drag and the effect of friction drag increase from increase of contact surface of flow with rectangular column has little effect on the increase of total drag. From, wedged column has the greatest drag coefficient at 45 relative to other columns as it has the greatest reference surface and elliptical column has the least drag coefficient due to pressure drag reduction.

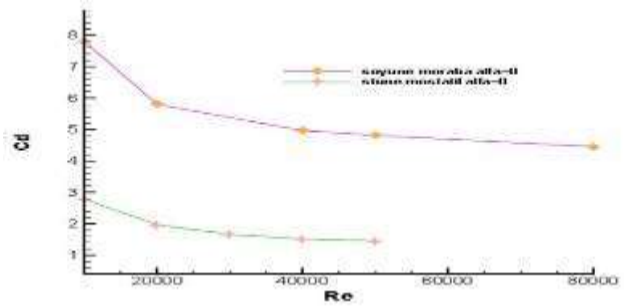

Fig: 6. change in square, elliptical and wedged column drag coefficient versus Reynolds number at attack angle 45

CONCLUSION

Fluid flow on the different shapes of column, square, rectangle, sharp-tip wedged-like , parabola and elliptic at different Reynolds` number were investigated .The contour of velocity, pressure, flow lines and eddy structure behind the columns are represented. in all columns, drag coefficient decreased with the increase of Reynolds` number. one of the important results of this project is stating that friction drag has little effect on total drag. For wedged column at 45 degrees, flow separation and flow non-recontact to surface have effect on reduction of drag coefficient.

CONFLICT OF INTEREST
The author declares having no competing interests.

ACKNOWLEDGEMENT
None.

FINANCIAL DISCLOSURE
None.

REFERENCES

[1] Laursen EM.[1956] Scour around bridge piers and abutments, Bulletin 4, Iowa highway research board, Iowa city,

[2] Laursen EM. [1956] Scour around bridge piers and abutments", Bulletin 4, Iowa highway research board, Iowa city

[3] Laursen EM. [1962]Scour at bridge crossings, transation ASCE, 127:166-180.

[4] Jones JS. [1984] Comparison of prediction equations for bridge pier and abutmentscour, Transportation research record 950, Second bridge Engineering Conference, 2: 202- 209

[5] Parol AC, Jones JS, Miller AC. [1989] Model study on the stability of riprap placed in local scour holes at bridge , Dept of Imterior, U.S. Geological survey,Water resources Divion office of water Data Cordination, pp.307-317.

[6] Ansari SA, Kothyari UC, Ramga KG. [2002] Influence of cohesion on scour around Bridge piers , Journal of Hydraulic Research, 40(6): 717-729.

[7] Baker CJ. [1980] Theoretical approach to prediction of local scour around bridge piers, Journal of Hydraulic Research, 18(1).

[8] Boehmler EM, Olimpio JR. [2000] Evaluation of pier – scour measurement me thods and pier scour prediction with observed scour mesurement at selected bridge sites in New Hampshire, 1995-98, Water Resources Investigation, Report 00-4183.

[9] Bozkus Z, Yildiz O. [2004] Effects of inclination of bridge piers on scouring depth, Journal of Hydraulic Engineering, 130(9):905-913.

[10] Breusers HNC. [1977] Local scour around cylindrical piers, Journal of Hydraulic Research, 15:211-215.

[11] Chang WY, Lai JS, Yen CL. [2004] Evolution of scour depth at circular bridge piers, Journal of Hydraulic Engineering, 130(9): 905-913.

[12] Chiew YM. [1992] Scour protection at bridge piers, Journal of Hydraulic Engineering, 118(9).

[13] Ettema R. [1980] Scour at bridge pier, Deprt of civil Engineering university of Auckland, New zealand, No. 216